Available online at www.sciencedirect.com
SCIENCE DIRECT®
Polymer 44 (2003) 7539–7544
polymer
www.elsevier.com/locate/polymer

Structure and dynamics in the amorphous region of natural rubber observed under uniaxial deformation monitored with solid-state ^{13}C NMR

Tsunenori Kameda, Tetsuo Asakura*

Department of Biotechnology, Tokyo University of Agriculture and Technology, Koganei, Tokyo 184-8588, Japan

Received 31 March 2003; received in revised form 22 July 2003; accepted 6 September 2003

Abstract

Solid-state ^{13}C NMR experiments were performed under uniaxial deformation of natural rubber to investigate the changes in the structural and dynamical behavior of the amorphous region induced by elongation. The structural change was detected as the change in the ^{13}C cross-polarization (CP) chemical shifts and line shapes. In addition, change in the CP ^{13}C peak intensity as a function of time was also observed and was used to monitor the change of the dynamical behavior with time in high resolution. The relationship between ^{13}C CP intensity and molecular dynamics under uniaxial deformation of natural rubber was examined by the ^{1}H magnetization decay behavior in the rotating frame and $^{1}H-^{13}C$ CP build-up curves. Although the strain-induced crystallization occurred at around 200% strain, the ^{13}C lineshapes showed no significant change in the orientation of the amorphous chains. On the other hand, the molecular dynamics of the amorphous chains was greatly affected even under lower extension, that is, the enhanced mobility of the chains was observed at 30% strain. This enhanced mobility induced by deformation decreased after the deformation was stopped.

Keywords: Natural rubber; Solid-state NMR; Uniaxial deformation

1. Introduction

Biopolymers, such as spider dragline silks, collagens and elastins, provide high elasticity [1]. This property makes such materials an extremely attractive candidate for numerous applications. As a result, there is considerable interest in the design of these materials as a guide to the commercial production of protein-based structural polymers. Although some biopolymers are known to show a typical response of rubber-like or entropy elasticity [2], understanding how the structure and mobility of molecules influence this amazing property is less advanced. One of the reasons for this lack of clarity is that the elastic property in biopolymers is derived from the amorphous regions. In general, detailed determinations of the molecular structure and mobility in the amorphous region by means of material characterization techniques such as X-ray diffraction analysis are considered difficult. However, solid-state NMR has an advantage over other techniques because of its ability to get both the molecular structure and dynamic information in the amorphous region [3–10]. Especially effective is the orientation-dependent solid-state NMR method which makes it possible to determine both the structure and dynamics for stretched or stretching polymers [5,7,8,11–23]. We have applied this method to the fibers and films of silk fibroins [11,12,15–19] and synthetic polymers [20–23]. The most noteworthy result was that the torsion angles of the glycine and alanine residues in *Bombyx mori* and *Samia cynthia ricini* silk fibers were determined with high precision [16–19]. More recently, strain inducible solid-state NMR equipment as shown in Fig. 1 was developed to monitor the structural and dynamical changes of the polymer and protein fibers under uniaxial deformation. This equipment was applied to monitoring change in the crystal transition from α to β forms of a biodegradable aliphatic polyester fiber, poly (tetramethylene succinate) (PTMS) as a function of tensile stress [5].

To explore the origin of the elastic property in biopolymers by means of solid-state NMR, pre-examination of how the elasticity influences the NMR spectra is necessary. As a model compound for pre-examination, vulcanized natural rubber was employed in this study. Vulcanized natural rubber is known as an exceptionally tough elastomer

* Corresponding author. Tel./fax: +81-42-383-7733.
E-mail address: asakura@cc.tuat.ac.jp (T. Asakura).

0032-3861/$ - see front matter © 2003 Elsevier Ltd. All rights reserved.
doi:10.1016/j.polymer.2003.09.048

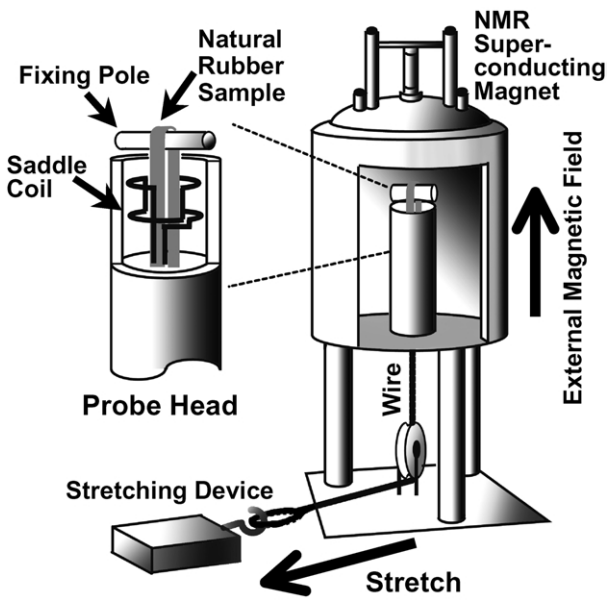

Fig. 1. Schematic diagram of equipment developed to monitor change in the solid-state NMR spectra of natural rubber under uniaxial deformation [5]. Each end of the rubber band was hooked onto a pole made from wood and Kevlar wire. The Kevlar wire was connected to the stretching device located away from the magnet. Stretching on the rubber sample was induced parallel to the static magnetic field at room temperature. The elongation rate was 30 mm/min.

because it has high elasticity, high tensile stress, large hysteresis loss, and crystallizes when stretched [3,24–29]. Recently, the strain-induced structural change of the natural rubber with X-ray diffraction analysis has been studied extensively by Toki, Murakami and their colleagues [24–26,28]. The high intensity of synchrotron X-rays and new image analysis methods made it possible to estimate mass fractions of strain-induced crystal and amorphous chains in both oriented and unoriented states during uniaxial deformation for natural rubber [25,26]. However, the lack of long-range order in the amorphous regions of natural rubber still precludes in-depth investigation by the X-ray diffraction technique [21]. On the other hand, solid-state NMR provides an advantage over other methods for studying the amorphous region of natural rubber [30,31]. Nishi and Chikaraishi measured the ^{1}H spin–spin relaxation time (T_2) for natural rubber under various strains by pulsed NMR [10]. They found that molecular motion is directly related to the draw ratio, and decreased with increasing deformation. The pulsed NMR measurement detects overall molecular dynamics. Although this technique is sometimes able to clearly distinguish the crystalline and amorphous parts, it was impossible to get site selective information. Moreover, no information on the orientation of the amorphous chain was obtained from this technique.

In this study, in order to investigate the effect of uniaxial deformation on the molecular orientation and dynamics in the amorphous region of the natural rubber, the strain inducible ^{13}C solid-state NMR experiment was performed.

2. Experimental section

We have investigated the commercially available elastic bands made from the natural rubber (Fig. 2(A)). The full length of the sample was 100 mm. As shown in Fig. 1, the end of the rubber band was hooked onto Kevlar wire, which connected it to the stretching device [5]. Stretching of the rubber sample was induced parallel to the static magnetic field of NMR at room temperature. The elongation rate was 30 mm/min. The stretching ratio was determined from the migration length of the mark on the sample before and after stretching.

All NMR experiments were performed on a Chemagnetics CMX Infinity 400 MHz spectrometer. A homemade probe with a 5-mm saddle coil and double tuning system for cross-polarization (CP) was used for strain inducible NMR.

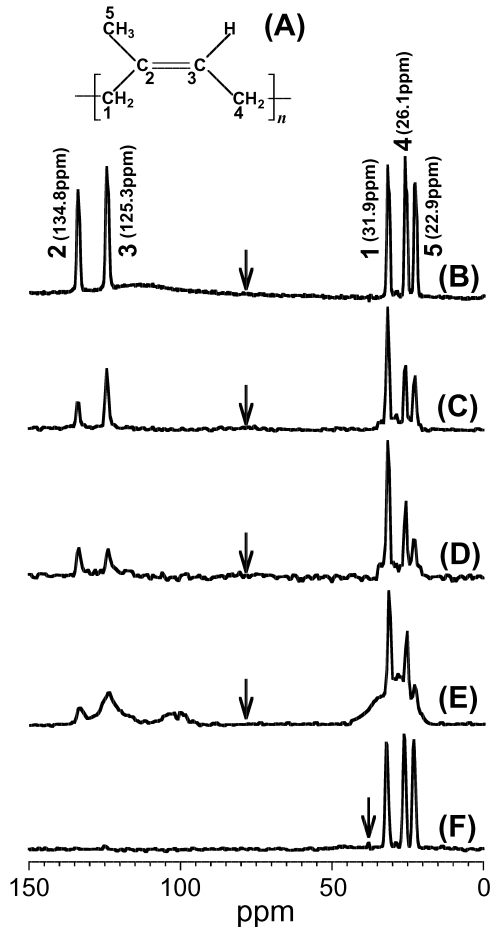

Fig. 2. (A): Structure of the repeat unit in *cis*-1,4-poly(isoprene). (B): ^{13}C direct polarization spectrum with ^{1}H decoupling for the unstretched natural rubber. (C): As in (B) but ^{13}C cross-polarization (CP) spectrum. (D): ^{13}C CP spectrum of 100% stretched natural rubber with the draw axis set parallel to the external magnetic field. (E): As in (D) but at 200% strain. The spin-locking power of $\omega_{^{13}C}/2\pi = \omega_{^{1}H}/2\pi$ during CP was 33 kHz for (C)–(E). (F): As in (C) but the spin-locking power $\omega_{^{13}C}/2\pi = \omega_{^{1}H}/2\pi$ during CP was 20 kHz and the position of rf irradiation was different with (B)–(E). Arrows indicate the positions of rf irradiation. The number of scans for each spectrum was over 1k times. Therefore, it continued to scan over 1 h for each spectrum.

The variable-temperature NMR experiments were carried out with a commercial CP/magic-angle spinning (MAS) probe with a 7.5 mm coil (produced by Chemagnetics). The spinning frequency was 4.0 kHz. A CW proton decoupling field strength of 28 kHz was used in all experiments. For the normal 90° single pulse sequence with the gated high-power decoupling experiments, a 90°-pulse width of 12.0 μs was employed. $^{1}H-^{13}C$ CP contacts of 22 or 30 kHz, and contact times from 0.1 to 35 ms were used. The repetition time was 1.5 s in all experiments. The ^{1}H magnetization was observed in the variable proton spin-locking time followed by $^{1}H \rightarrow {}^{13}C$ CP experiments. The CP contact time was set at 4 ms with a spin-locking field strength of 20 kHz. The chemical shifts of all ^{13}C spectra were determined by taking the carbon of solid adamantane as an external reference standard.

3. Results and discussion

3.1. Effects of uniaxial deformation on the chain orientation

A normal 90° single pulse sequence with gated high-power decoupling can be used to examine the highly mobile (amorphous) regions in natural rubber (Fig. 2(B)). Three aliphatic (22.9, 26.1, and 31.9 ppm) and two olefinic peaks (125.3 and 134.8 ppm) from the mobile carbons in the natural rubber (cf. Fig. 2(A)) can be identified in the spectra. These chemical shifts are in agreement with the isotropic chemical shifts observed in the NMR spectrum with MAS (data not shown). These results indicate that the motions of the carbons, originating from peaks 1–5 in Fig. 2(B), are fast enough to average out the chemical shift anisotropies.

A series of ^{13}C CP NMR spectra of natural rubber as a function of strain is shown in Fig. 2(C)–(E). The CP contact time was set at 4 ms. The signal of the immobile component is enhanced by CP. From Fig. 2(C)–(E), profound changes in the line widths of the peaks 1–5 were observed, which is considered to reflect the decrease in segmental motion with increasing strain. At 200% strain, new broad signals that can be assigned to the crystalline state were observed on both the high- and low-field sides of the peaks originating from the amorphous region (Fig. 2(E)). This result is in agreement with the result obtained by Toki, Murakami and their colleagues [24–26], have shown, by means of wide-angle X-ray techniques, that strain-induced crystallization occurs at around 200% strain. When the drawing axis is parallel to the external magnetic field ($\mathbf{B}_0$), the observed chemical shifts and line shapes depend on the angle between the molecular orientation axis and $\mathbf{B}_0$. With increasing uniaxial strain, the positions for peaks 1–5 in Fig. 2(C)–(E) that come from the amorphous region, were virtually unchanged and remained at the isotropic chemical shifts (Fig. 2(B)). These results suggest that chain segmental motion would disrupt molecular orientation and that amorphous chains remained unoriented under uniaxial deformation. Its chain segmental motional rate is fast enough to average the chemical shift anisotropy, i.e. more than kHz order. Toki, Murakami and their colleagues also pointed out in an in situ synchrotron X-ray diffraction study that only a few percent of the amorphous chains were oriented and the rest of the chains were in the crystalline phase even at a large strain [26].

Because of the requirement of a longer spin-locking time (>35 ms) for CP in this experiment, the spin-locking power during CP was kept down to 20 kHz. Such low spin-locking power would induce the mismatched Hartmann–Hahn condition causing the offset effect to become more serious. When the Hartmann–Hahn condition is not fulfilled (that is the mismatched condition), the CP efficiency will be reduced. Therefore, in the case of rf irradiation was applied in the vicinity of the aliphatic region, such that only the aliphatic carbon peaks were detectable as shown in Fig. 2(F). For the remainder for this paper above condition will be used and the focus will be on the aliphatic region.

3.2. Chain mobility of the amorphous region in the unstretching state

The ^{1}H magnetization decays behavior observed in variable ^{1}H spin-locking times followed by $^{1}H \rightarrow {}^{13}C$ CP experiments at different temperatures are shown in Fig. 3. It was found that the decay curves of ^{1}H magnetization grew steep with decreasing temperature. This result indicates that the ^{1}H $T_{1\rho}$ relaxation is remarkably sensitive to local motion, and monotonically decreases when the flexibility of the chains is decreased. Note that the variable-temperature

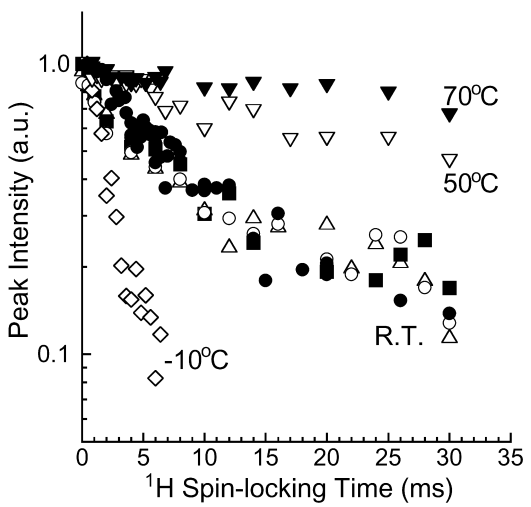

Fig. 3. Semilogarithmic plots of the ^{13}C-edited ^{1}H spin-locking time dependence of the aliphatic carbons of 31.9 ppm (○), 26.1 ppm (■) and 22.9 ppm (△) in the unstretched natural rubber at room temperature. The temperature dependences of the ^{1}H magnetization decay at −10 °C (◇), room temperature (●), 50 °C (▽), and 70 °C (▼) are also indicated, which were observed by means of the commercial MAS probe in the spinning frequency at 4.0 kHz. The proton magnetization is kept in spin-locking for a variable period of time before it is cross-polarized to the carbon nuclei. The spin-locking power of $\omega_{1H}/2\pi$ was 20 kHz.

experiments in Fig. 3 were carried out using the commercial MAS probe with a spinning frequency of 4.0 kHz. Although the handmade strain-inducible probe was only available for the detection of the ^{1}H decays at room temperature, it can be seen that two probes gave the similar decaying slopes at this temperature. Therefore, the effect of MAS on the ^{1}H $T_{1\rho}$ relaxation is negligible.

Moreover, the fact that non-linear relations between the logarithm of the peak intensities and the variable ^{1}H spin-locking evolution time (non-exponential decay) in Fig. 3 were observed indicates that the motional heterogeneity would exist in the amorphous region of natural rubber. The ^{1}H $T_{1\rho}$ relaxation for the cross-linked parts of the matrix is considerably shorter than that for the uncross-linked chains. Consequently, natural rubber that is composed with a mixture of cross-linked and uncross-linked chains appears to have a multi-exponential $T_{1\rho}$ decay.

Fig. 4 shows the variable temperature studies for the changes in the ^{13}C signal intensities of the aliphatic carbons as a function of contact time (contact-time build-up curve) under MAS. The peak intensities reach a maximum prior to decreasing with increasing contact time. Similar variable contact time curves have been obtained in all of the aliphatic carbons at a given temperature. The increase in the ^{13}C intensities at short contact times is dominated by the CP rate ($1/T_{CH}$), whereas the decrease in the intensities for the longer contact times by the ^{1}H spin-lattice relaxation rate ($1/T_{1\rho}$) in the rotating frame [6,32]. From Fig. 4, it can be seen that the CP rate in the rising part decreased, i.e. T_{CH} increased with increasing temperature. This result demonstrates that the T_{CH} of natural rubber differs among mobile and rigid components, similar to ^{1}H $T_{1\rho}$, and increases when the flexibility of the chains is increased.

The CP build-up curves in Fig. 4(A) show the presence of multi-components, because there are plateaus around maximum intensities. This result indicates the existence of a heterogeneous structure in natural rubber, which is consistent with the result of the ^{1}H magnetization decay behavior in the rotating frame, as shown in Fig. 3.

3.3. Effects of uniaxial deformation on chain mobility in the amorphous region

Fig. 5 shows the ^{1}H spin-locking time dependence of aliphatic carbon of 31.9 ppm at 30% strain, monitored immediately after stopping elongation, and after it passed for more than 60 min, together with the fitting curve of the plot in an unstretched state at room temperature in Fig. 3. The decay observed immediately after stopping the deformation at 30% strain had a slower rate than that observed both before stretching and after 60 min. The differential in these decays is attributed to the difference in their molecular dynamics. The long ^{1}H $T_{1\rho}$ relaxation is consistent with a fast motion, since ^{1}H $T_{1\rho}$ increases with increasing temperature as shown in Fig. 3. Therefore, it is considered that the mobility of the amorphous chains was enhanced by the deformation, and its enhanced mobility decreased with time once deformation was stopped. If such motional changes occurred, it would be expected that T_{CH} would also be affected, thus causing alteration of the CP build-up curve. This possibility was investigated by means of variable CP experiments detailed below.

Fig. 6 shows the plots of CP peak intensities for aliphatic

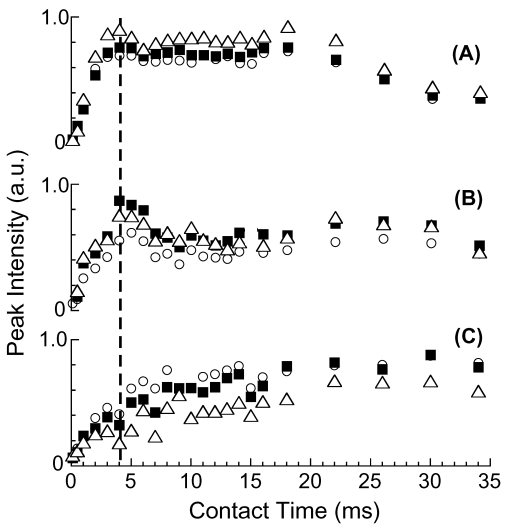

Fig. 4. Plots of the variation of ^{13}C peak intensities (arbitrary units) of aliphatic carbon peaks of 31.9 ppm (○), 26.1 ppm (■) and 22.9 ppm (△) with contact time in 0% strain (unstretching); at room temperature (A), 50 °C(B), and 70 °C (C). The dotted line represents a contact time of 4 ms. The spectra (B) and (C) were obtained with the commercial CP/MAS probe, and spinning speed was 4 kHz. The number of scans for obtaining each plot was 16 times.

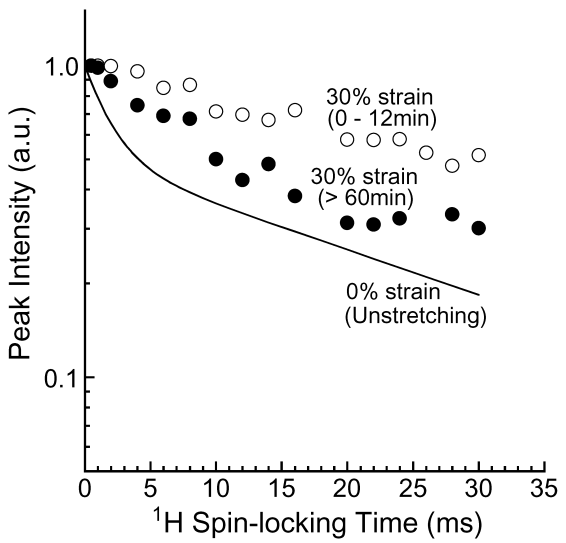

Fig. 5. Semi logarithmic plots of the ^{13}C-edited ^{1}H spin-locking time dependence of aliphatic carbon of 31.9 ppm at 30% strain, monitored immediately after stopping elongation (○), and after it passed for more than 60 min (●). The solid curve indicates the fitting of ^{1}H magnetization decay at 0% strain (see Fig. 3). The number of scans for obtaining each plot was 16 times.

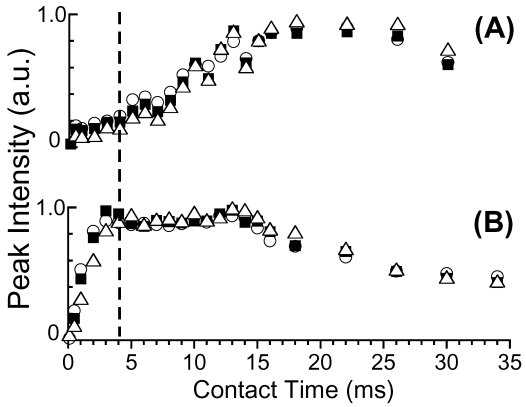

Fig. 6. Contact time dependent peak intensities of the aliphatic carbons of 31.9 ppm (○), 26.1 ppm (■) and 22.9 ppm (△), for natural rubber, at elapsed time from 0 to 20 min (A), and from 60 to 80 min (B) immediately after stopping the deformation at 30% strain. The dotted line represents a contact time of 4 ms. The number of scans for obtaining each plot was 16 times.

carbons as a function of contact time. The correction in the plots of Fig. 6(A) started immediately after stopping the deformation at 30% strain. Note that the motional change occurred continuously during the data collection. As a result, the CP curves in Fig. 6(A) have an unexpected shape, e.g. although the rising in the intensities of short contact time by T_{CH} effect is convexly curved theoretically, concave curves were observed. Therefore, a quantitative analysis of the T_{CH} value in Fig. 6(A) would be difficult. However, some semi-quantitative observations can be made. For example, the CP curves in Fig. 6(A) not only seem to be different from Fig. 6(B), but also from Fig. 4(A). Namely, the rate of initial rising and decaying in the longer contact time of peak intensities in Fig. 6(A) are slower than those in Fig. 6(B) and Fig. 4(A). This observation indicates that the T_{CH} and $T_{1\rho}$ values observed immediately after stopping the deformation increased. On the other hand, the behavior of CP curves in Fig. 6(B) is similar to that in Fig. 4(A). Based on the fact that T_{CH} and ^{1}H $T_{1\rho}$ increases with increasing mobility as shown in Fig. 4 and Ref. [33], the elongation enhanced the mobility of the amorphous chains, and its enhanced mobility was restricted when the deformation was stopped. These results are consistent with above data (see Fig. 5).

Now, we focus on the peak intensities at the contact time of 4 ms in Fig. 4(A) and Fig. 6(A) and (B). Those intensities are significantly different from each other due to the difference in contribution of the molecular motion to the CP efficiency. Therefore, at a given contact time of 4 ms, it can be expected that the peak intensities will decrease remarkably when the sample is drawn up to 30% strain, and then increase gradually when the sample length is fixed at 30% strain. This expectation can be verified through the following experiment.

When the deformation was stopped at 30% strain and the length was fixed, the effect of time on the CP peak intensities of aliphatic carbons was studied by measuring the peak height at time intervals of 48 s immediately after fixed at 30% strain (Fig. 7(B)), together with the peak intensities in the equilibrium state at 0% strain (Fig. 7(A)). By comparing Fig. 7(A) and (B), it can be seen that immediately after stopping the deformation at 30% strain, the CP peak intensities for the aliphatic carbons dropped significantly. These intensity losses were linearly recovered when the deformation was stopped. As predicted above, the remarkable loss and increase of peak intensities are considered to be due to the enhancement and restriction of the mobility in the amorphous region, respectively. The fact that the loss in the intensity was mostly recovered in 900 s indicates that the enhanced mobility caused by the 30% stretching decayed within 900 s. This experiment indicated that the dynamic change under uniaxial deformation of natural rubber was successfully monitored in high time resolution by CP ^{13}C peak intensity. Note that the intensity loss was not due to a drawn out of the sample from coil volume. Such disturbance was estimated to give a loss in intensity of at most 20%. This estimate was checked by a 90° single pulse sequence experiment.

Recently, similar behavior was reported by Loo et al. [13]. They examined the effect of uniaxial deformation on the chain mobility in the amorphous region of the semi-crystalline nylon 6 with solid-state deuterium NMR. Near the glass transition temperature, the deformation induced the enhancement of the mobility in the amorphous region up to the yield point of nylon 6, and its enhanced mobility decayed when the deformation was stopped. Loo et al. explained the effect of the deformation on the change in the mobility using the Robertson model [34] for glassy polymers near the glass transition temperature. Robertson assumed that under shear stress the population of flexed segments increased transiently, leading to an increase in the 'structural temperature' of the solid. When the deformation

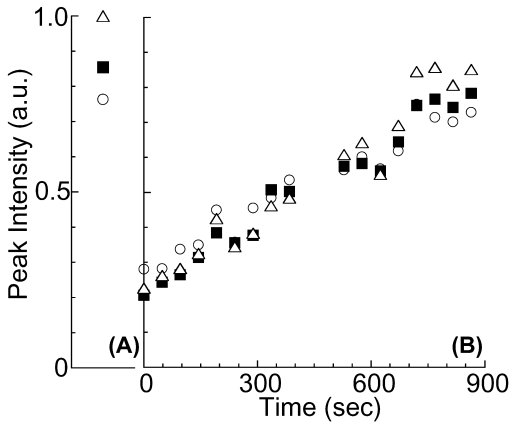

Fig. 7. (A): The CP intensities of the aliphatic carbon peaks of 31.9 ppm (○), 26.1 ppm (■) and 22.9 ppm (△) in equilibrium state at 0% strain. (B): The effect of time on the CP signal intensities of aliphatic carbon peaks, measured at time intervals of 48 s. This interval is determined by multiplying the 3 s recycle delay by 16 scans. The CP contact time was set at 4 ms.

was stopped, some of the liquid-like character reverted back to a solid-like state, which resulted in a decreased amount of mobility. The Robertson model could also be applicable to natural rubber under deformation at room temperature, because room temperature is above the glass transition temperature for natural rubber, which is almost −70 °C.

Furthermore, we considered that the enhancement of chain mobility during deformation causes the rising temperature because of the Gough–Joule effect. Such rising temperature will fall eventually due to the heat transfer from the rubber chains to the surroundings, which in turn induces a decrease in enhanced mobility when the sample is fixed to a constant length. This consideration is consistent with an explanation of the entropic mechanism of rubber elasticity. In addition, stress relaxation may also be considerable when stretching is stopped. And this would induce motional enhancement of the molecular chain due to an increase of entropy. However, contrary to this expectation, the chain mobility decreased with time when the sample length is fixed at 30% strain as described above. Therefore, the effect of the stress relaxation on the chain mobility appears to be negligible.

4. Conclusion

We have performed solid-state ^{13}C NMR experiments of natural rubber under uniaxial deformation. These experiments have provided vital information about chain orientation and dynamics during deformation in the amorphous region. Deformation gave no significant change in the orientation of the amorphous chains even at 200% strain, whereas the molecular dynamics depended strongly on deformation at a lower elongation of only 30% strain. Enhanced mobility of the amorphous chain introduced by uniaxial deformation was clarified using both the ^{1}H magnetization decay behavior in the rotating frame, and CP build-up curves. This enhanced mobility decayed once the deformation was stopped. Moreover, the dynamic change with time under deformation was successfully monitored in high time resolution by the CP ^{13}C peak intensity.

Finally, we have demonstrated that the strain-inducible solid-state NMR is a useful tool for analyzing molecular orientation and dynamics in the amorphous region of natural rubber. The time dependence of the CP peak intensity gives NMR spectroscopy a powerful advantage over other spectroscopic techniques for studying motion. That information is of fundamental importance and provides the basis of a better understanding of rubbery polymer behavior.

Acknowledgements

The authors would like to thank to Dr Teruaki Fujito and Mr Mamoru Imanari, JEOL DATUM LTD, for their technical assistances. We are grateful to Dr Hiroki Uehara, Gunma University, for helpful discussion. T.A. acknowledges the supports of the Program for Promotion of Basic Research Activities for Innovative Biosciences, Japan.

References

[1] Gosline JM, Guerette PA, Ortlepp CS, Savage KN. J Exp Biol 1999; 202:3295–303.
[2] Gosline JM, Denny MW, DeMont ME. Nature 1984;309:551–2.
[3] Kariyo S, Stapf S. Macromolecules 2002;35:9253–5.
[4] Kameda T, Asakura T. Annu Rep NMR Spectrosc 2002;46:101–49.
[5] Kameda T, Kobayashi M, Yao J, Asakura T. Polymer 2001;43: 1447–51.
[6] Sotta P. Macromolecules 1998;31:3872–9.
[7] Weigand F, Spiess HW. Macromolecules 1995;28:6361–4.
[8] Schaefer DJ, Schadt RJ, Gardner KH, Gabara V, Allen SR, English AD. Macromolecules 1995;28:1152–8.
[9] Hansen MT, Boeffel C, Spiess HW. Colloid Polym Sci 1993;271: 446–53.
[10] Nishi T, Chikaraishi T. J Macromol Sci (Phys) 1981;B19:445–57.
[11] Kameda T, Ohkawa Y, Yoshizawa K, Nakano E, Hiraoki T, Ulrich AS, et al. Macromolecules 1999;32:8491–5.
[12] Kameda T, Ohkawa Y, Yoshizawa K, Naito J, Ulrich AS, Asakura T. Macromolecules 1999;32:7166–71.
[13] Loo LS, Cohen RE, Gleason KK. Science 2000;288:116–9.
[14] Asakura T, Demura M. In: Ando I, Asakura T, editors. Solid state NMR of polymers. Amsterdam: Elsevier; 1998. p. 307.
[15] Nicholson LK, Asakura T, Demura M, Cross TA. Biopolymers 1993; 33:847–61.
[16] Asakura T, Minami M, Shimada R, Demura M, Osanai M, Fujito T, et al. Macromolecules 1997;30:2429–35.
[17] Demura M, Minami M, Asakura T, Cross TA. J Am Chem Soc 1998; 120:1300–8.
[18] Demura M, Yamazaki Y, Asakura T, Ogawa K. J Mol Struct 1998; 441:155–63.
[19] Asakura T, Ito T, Okudaira M, Kameda T. Macromolecules 1999;32: 4940–6.
[20] Asakura T, Yeo J-H, Demura M, Itoh T, Fujito T, Imanari M, et al. Macromolecules 1993;26:6660–3.
[21] Asakura T, Demura M, Nishikawa N. Annu Rep NMR Spectrosc 1997;34:301–46.
[22] Ito T, Yamaguchi Y, Watanabe H, Asakura T. J Appl Polym Sci 2001; 80:2376–82.
[23] Ito T, Maruhashi Y, Demura M, Asakura T. Polymer 1999;41: 859–66.
[24] Toki S, Fujimaki T, Okuyama M. Polymer 2000;41:5423–9.
[25] Murakami S, Senoo K, Toki S, Kohjiya S. Polymer 2002;43:2117–20.
[26] Toki S, Sics I, Ran S, Liu L, Hsiao BS, Murakami S, et al. Macromolecules 2002;35:6578–84.
[27] Callaghan PT, Samulski ET. Macromolecules 1997;30:113–22.
[28] Trabelsi S, Albouy P-A, Rault J. Macromolecules 2002;35:10054–61.
[29] Rubinstein M, Panyukov S. Macromolecules 2002;35:6670–86.
[30] Fechete R, Demco DE, Bluemich B. Macromolecules 2002;35: 6083–5.
[31] Whittaker AK. Annu Rep NMR Spectrosc 1997;34:105–83.
[32] Schaefer J, Stejskal EO, Buchdahl R. Macromolecules 1977;10: 384–405.
[33] Fulber C, Demco DE, Blumich B. Solid State Nucl Magn Reson 1996; 6:213–23.
[34] Robertson RE. J Chem Phys 1965;44:3950–6.